Journal of Engineering Mathematics, Vol. 3, No. 2, April 1969
Wolters-Noordhoff Publishing – Groningen
Printed in the Netherlands

Solid Rectangular and T-Shaped Conductors in Semi-Closed Slots

D. E. JONES
Magnet Computer Bureau, G.E.C. (Eng.), Witton, Birmingham 6, England

N. MULLINEUX AND J. R. REED
Department of Mathematics, The University of Aston in Birmingham, Birmingham 4, England

R. L. STOLL
Department of Electrical Engineering, The University of Southampton, Southampton, England

(Received September 20, 1968)

SUMMARY
Previous methods of calculating the internal impedance of rectangular and T-shaped conductors have made arbitrary assumptions about the form of the magnetic field. These have led to inconsistencies. A method is developed which necessitates less restrictive assumptions, thereby removing the inconsistencies. Results are compared for typical conductor sizes.

List of symbols

a, b, c, d	= dimensions of conductor or slot
J	= current density
E	= electric field strength
V	= scalar potential
I	= current (r.m.s.) in conductor
B	= flux density
H	= magnetic field strength with components H_x, H_y in the x, y coordinate directions respectively
L	= inductance/unit length
R	= resistance/unit length
A'	= vector potential
A	= modified vector potential
A^*, A^{**}	= single and double cosine transforms of A
σ	= conductivity of conductor
μ	= relative permeability of conductor
ω	= angular frequency
α^2	$= j\omega\mu\mu_0\sigma$
m, n	= transform parameters
C_m	$= \{(m\pi/c)^2+\alpha_1^2\}^{\frac{1}{2}}$
D_n	$= \{(n\pi/d)^2+\alpha_2^2\}^{\frac{1}{2}}$
P_m, Q_n	= coefficients
K	= constant of integration
Re, Im	= real, imaginary parts of complex function respectively.

1. Introduction

In the attempt to design more effective machines, problems previously investigated in a rather approximate manner are now being reconsidered and more complete solutions sought. This is no criticism of the earlier investigators who had of necessity to make simplifying approximations in order to produce results at all. For example if Putman [1] could have made use of present generation computers then his approach to the problem of the current distribution in a T-bar conductor in an iron slot would probably not have been based on the assumption that the flux throughout the slot was unidirectional.

More recently Swann and Salmon [2] have used modern facilities to remove this assumption in the conductor for the case of rectangular conductors in semi-enclosed slots.

In the present investigation Putman's original problem of a T-bar conductor is reconsidered. This problem contains that of Swann and Salmon as a limiting case and indeed attempts to overcome an inconsistency in that their expression for J leads to a non-zero flux density up the neck of the slot, contrary to the hypothesis of an entirely transverse flux density in this region.

The solution is obtained in terms of vector potentials in the two rectangular regions of the T-bar (see Figure 1), and the crux of the method is to match these vector potentials along the common boundary. Here use is made of a technique recently introduced into field analysis by Midgley and Smethurst [3]. Again the effective use of the technique presupposes the use of automatic computation.

Recently Silvester [4] has formulated a method of solution for a conductor of arbitrary shape in any shape of slot. However rectangular and T-shaped conductors occur frequently in practice and the method proposed here has the advantage for these cases of using considerably less computer time.

2. T-Shaped Conductor

In this investigation the object is to obtain the current distribution in, and the effective impedance of, a T-bar conductor in a T-section slot. The following assumptions are made:

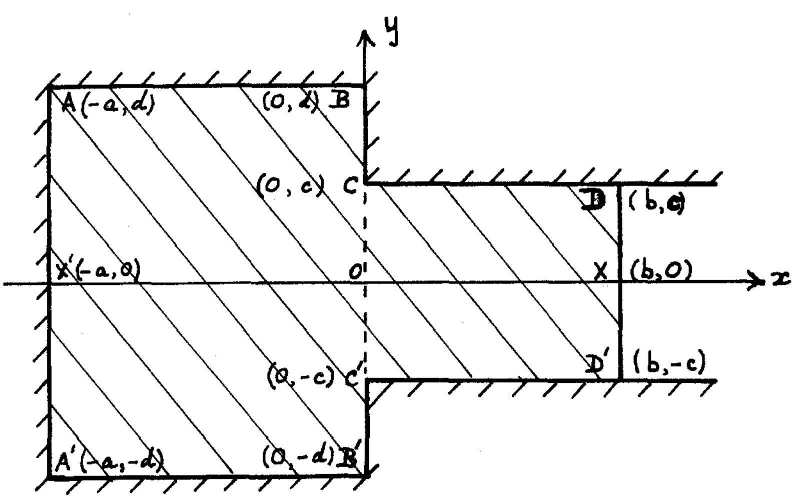

Figure 1. T-bar conductor.

a) the conductor completely fills the slot as shown in Figure 1 (this is generally valid since even if the conductor is insulated the electrical stresses are low and only thin insulation is required),

b) the iron is of infinite permeability and is laminated so that eddy-currents in the iron may be neglected,

c) outside the conductor, beyond DD′, the natural assumption would be that the flux is directed across the slot perpendicularly to its walls i.e. $H_x = 0$ and H_y is constant and equal to $I/(2c)$. It transpires however that in solving the field problem within the conductor it is impossible to specify a priori *both* $H_x = 0$ and $H_y = I/(2c)$ on DD′, for then the problem would be mathematically overdefined. The procedure here adopted is to specify that $H_y = I/(2c)$ on DD′, solve the problem and then check that H_x is indeed small compared with H_y.

It is in the last assumption that the present approach differs from that of Putman who assumed $H_x = 0$ throughout the slot.

2.1) *Formulation of the problem*

From Maxwell's equations we have that in terms of instantaneous quantities

$$\nabla^2 A' = -\mu\mu_0 \boldsymbol{J} \tag{1}$$

$$\boldsymbol{J} = \sigma \boldsymbol{E} \tag{2}$$

$$\boldsymbol{E} + \frac{\partial A'}{\partial t} = \nabla V \tag{3}$$

The current distribution is such that the potential V is constant over the cross-section of the conductor so that all vectors are in the axial direction of the slot. Assuming a sinusoidal variation with time the quantities in equations (1), (2) may be replaced by r.m.s. phasors and equation (3) becomes

$$E + j\omega A' = \text{constant} = \beta, \text{ say} \tag{4}$$

and with the substitution

$$A = A' + j\beta/\omega \tag{5}$$

equation (4) reduces to

$$E = -j\omega A \tag{6}$$

and on substitution into the phasor equivalents of equations (1), (2) there results

$$\frac{\partial^2 A}{\partial x^2} + \frac{\partial^2 A}{\partial y^2} = j\mu\mu_0 \sigma\omega A = \alpha^2 A \tag{7}$$

where

$$\alpha^2 = j\mu\mu_0 \sigma\omega .$$

The definitions of A', A yield

$$\boldsymbol{B} = \nabla \wedge \boldsymbol{A}' = \nabla \wedge \boldsymbol{A}$$

so that, under the assumptions listed, the boundary conditions become

$$\frac{\partial A}{\partial x} = 0 \qquad \text{on AA}', \text{BC}', \text{B}'\text{C}'$$

$$\frac{\partial A}{\partial x} = -\frac{\mu_0 I}{2c} \qquad \text{on DD}'$$

$$\frac{\partial A}{\partial y} = 0 \qquad \text{on AB, A}'\text{B}', \text{CD, C}'\text{D}'.$$

Further it follows from symmetry that on X′X, $H_x = 0$, i.e. $\partial A/\partial y = 0$. Consequently the solution need only be obtained for the half-slot $y \geqq 0$.

2.2) *Solution for the vector potential*

The method of solution employed is to obtain the solutions in each of the regions OCDX, X′ABO in terms of the unknown $\partial A/\partial x$ along the common boundary OC, in the form of infinite series. Since, however, the coefficients in the series remain to be determined the series are truncated to N terms and the resulting approximations to A in the two regions equated along OC and to $\partial A/\partial x$ along OB, so providing the requisite number of equations for the determination of the coefficients in the truncated series. Clearly the method is an approximation but the degree of approximation can be checked by truncating at different values of N and comparing the final results. This practical approach to the estimation of accuracy seems preferable to a theoretical one, since in the latter, difficulties arise from the unknown dependence of P_m, Q_n on m, n respectively.

In region 1, OCDX

$$\frac{\partial^2 A_1}{\partial x^2} + \frac{\partial^2 A_1}{\partial y^2} = \alpha_1^2 A_1 \tag{8}$$

$\partial A_1/\partial y = 0$ on CD, OX; $\partial A_1/\partial x = -\mu_0 I/2c$ on DX and we set $\partial A_1/\partial x = f(y)$, say, on OC so that taking the finite cosine transform of equation (8) w.r.t. y there results

$$\frac{d^2 A_1^*}{dx^2} - \frac{m^2\pi^2 A_1^*}{c^2} = \alpha_1^2 A_1^* , \tag{9}$$

where

$$A_1^* = \int_0^c A_1 \cos(m\pi y/c)\, dy$$

and at $x=0$,

$$\frac{dA_1^*}{dx} = \int_0^c f(y) \cos(m\pi y/c)\, dy = P_m \text{ say}$$

at $x=b$,

$$\frac{dA_1^*}{dx} = -\frac{\mu_0 I}{2}\delta_{m,0}$$

where $\delta_{m,0}$ is Kronecker's delta $= 1$ if $m=0$ and 0 if $m \neq 0$.

Application of the finite cosine transform w.r.t. x to equation (9) yields

$$A_1^{**}(m, n) = -\frac{P_m + (-1)^n \mu_0 (I/2)\delta_{m,0}}{(m\pi/c)^2 + (n\pi/b)^2 + \alpha_1^2} . \tag{10}$$

The inverse transform is given by [5]

$$\begin{aligned} A_1 = \frac{A_1^{**}(0,0)}{bc} &+ \frac{2}{bc}\sum_{m=1}^{\infty} A_1^{**}(m,0)\cos(m\pi y/c) + \\ &+ \frac{2}{bc}\sum_{n=1}^{\infty} A_1^{**}(0,n)\cos(n\pi x/b) + \\ &+ \frac{4}{bc}\sum_{m=1}^{\infty}\sum_{n=1}^{\infty} A_1^{**}(m,n)\cos(m\pi y/c)\cos(n\pi x/b) \end{aligned} \tag{11}$$

so that inserting the values for A_1^{**} from equation (10) and using the expression

$$\sum_{n=-\infty}^{\infty} \frac{(-1)^n \cos(n\pi x/b)}{(n\pi/b)^2 + \gamma^2} = \frac{b}{\gamma}\frac{\cosh \gamma x}{\sinh \gamma b} \tag{12}$$

to sum over n, there results

$$\begin{aligned} -A_1 = \frac{\mu_0 I}{2c\alpha_1}\frac{\cosh(\alpha_1 x)}{\sinh(\alpha_1 b)} &+ \frac{P_0}{c\alpha_1}\frac{\cosh\{\alpha_1(b-x)\}}{\sinh(\alpha_1 b)} + \\ &+ \frac{2}{c}\sum_{m=1}^{\infty}\frac{P_m\cos(m\pi y/c)}{C_m}\frac{\cosh\{C_m(b-x)\}}{\sinh(C_m b)} \end{aligned} \tag{13}$$

where $C_m^2 = (m\pi/c)^2 + \alpha_1^2$.

In the same way in region 2, X'ABO

$$-A_2 = \frac{Q_0}{d\alpha_2}\frac{\cosh\{\alpha_2(a+x)\}}{\sinh(\alpha_2 a)} + \frac{2}{d}\sum_{n=1}^{\infty}\frac{Q_n\cos(n\pi y/d)}{D_n}\frac{\cosh\{D_n(a+x)\}}{\sinh(D_n a)} \tag{14}$$

where

$$Q_n = -\int_0^c f(y)\cos(n\pi y/d)\,dy$$

and

$$D_n^2 = (n\pi/d)^2 + \alpha_2^2 .$$

It remains to determine the P_m, Q_n and to this end the infinite summations in equations (13), (14) are truncated to N terms.

Then at $x=0$, $\partial A/\partial x$ can be represented both as $\partial A_2/\partial x$ over $0<y<d$ and as $\partial A_1/\partial x$ for $0<y<c$ together with $\partial A_1/\partial x=0$ for $c<y<d$ so that

$$\int_0^d \left.\frac{\partial A_2}{\partial x}\right|_{x=0}\cos(n\pi y/d)\,dy = \int_0^c \left.\frac{\partial A_1}{\partial x}\right|_{x=0}\cos(n\pi y/d)\,dy$$

and substituting for $\partial A_1/\partial x$, $\partial A_2/\partial x$ at $x=0$ from the truncated forms of equations (13), (14) and carrying out the integration yields

$$\left.\begin{aligned} &-Q_0 = P_0 \\ &Q_n + P_0\frac{\sin(n\pi c/d)}{(n\pi c/d)} + \frac{1}{c}\sum_{m=1}^{N} k(m,n)P_m = 0, \quad 1\leqq n\leqq N \end{aligned}\right\} \tag{15}$$

where

$$k(m,n) = \begin{cases} \dfrac{\sin\{(m/c-n/d)\pi c\}}{(m/c-n/d)\pi} + \dfrac{\sin\{(m/c+n/d)\pi c\}}{(m/c+n/d)\pi} & \text{if } \dfrac{m}{c}\neq\dfrac{n}{d}, \\ c \quad \text{if } \dfrac{m}{c}=\dfrac{n}{d}. \end{cases}$$

Similarly at $x=0$, $A_1=A_2$ over $0<y<c$ so that

$$\int_0^c A_1\cos(m\pi y/c)\,dy = \int_0^c A_2\cos(m\pi y/c)\,dy$$

and the same procedure leads to, for $m=0$

$$\frac{\mu_0 I}{2\alpha_1}\frac{1}{\sinh(\alpha_1 b)} + \frac{P_0}{\alpha_1}\coth(\alpha_1 b) = \frac{cQ_0}{d\alpha_2}\coth(\alpha_2 a) + \frac{2}{d}\sum_{n=1}^{N}\frac{Q_n\sin(n\pi c/d)}{D_n(n\pi/d)}\Big/\coth(D_n a) \tag{16}$$

and for $1\leqq m\leqq N$

$$\frac{P_m}{C_m}\coth(C_m b) = \frac{1}{d}\sum_{n=1}^{N} k(m,n)\frac{Q_n}{D_n}\coth(D_n a). \tag{17}$$

Equations (15), (16), (17) provide $2N+2$ equations from which the coefficients P_m, $0\leqq m\leqq N$ and Q_n, $0\leqq n\leqq N$ may be determined as indicated in Appendix 8.1. Insertion of these coefficients in the truncated forms of equations (13), (14) yields approximations to A throughout the conductor. The degree of approximation can be made as close as desired by increasing N. The choice of N is discussed briefly in Appendix 8.2.

The current density follows immediately from equations (2), (6) as

$$J = -j\omega\sigma A . \tag{18}$$

2.3) *Effective impedance*

Taking the r.m.s. value for I, the complex power, P, per unit length can be written in terms of Poynting's vector as

$$P = \int_C (\boldsymbol{E} \wedge \tilde{\boldsymbol{H}}) \cdot \boldsymbol{n}\, dl = -j\omega \int_C (\boldsymbol{A} \wedge \tilde{\boldsymbol{H}}) \cdot \boldsymbol{n}\, dl\,, \tag{19}$$

where C is the boundary of the conductor, $\boldsymbol{n}$ is a unit vector perpendicular to C and $\tilde{\boldsymbol{H}}$ is the conjugate complex of $\boldsymbol{H}$. Only the tangential component of $\boldsymbol{H}$ gives non-zero components in the scalar triple product in the integrand of equation (19) and this is zero everywhere except on D′D (Figure 1) where it has the value $I/(2c)$ so that equation (19) reduces to

$$P = -\frac{j\omega I}{2c} \int_{-c}^{c} A_1 \bigg|_{x=b} dy\,. \tag{20}$$

$A_1|_{x=b}$ is obtained from the truncated form of equation (13) so that carrying out the integration in equation (20), and making use of the relation

$$P = I^2(R + jX)$$

where R, X are the effective resistance and reactance there results

$$R + jX = \frac{j\omega}{2c\alpha_1} \left\{ \mu_0 \coth(\alpha_1 b) + \frac{2P_0}{I} \frac{1}{\sinh(\alpha_1 b)} \right\}. \tag{21}$$

3. Rectangular Conductor

It might appear that the rectangular conductor shown in Figure 2 is a special case of the T-bar of the previous section. However, if the boundary conditions are considered in more detail a potential source of inconsistency is revealed.

Physically it is clear that at some distance along the neck of the slot say $x \geqq \xi$ then effectively

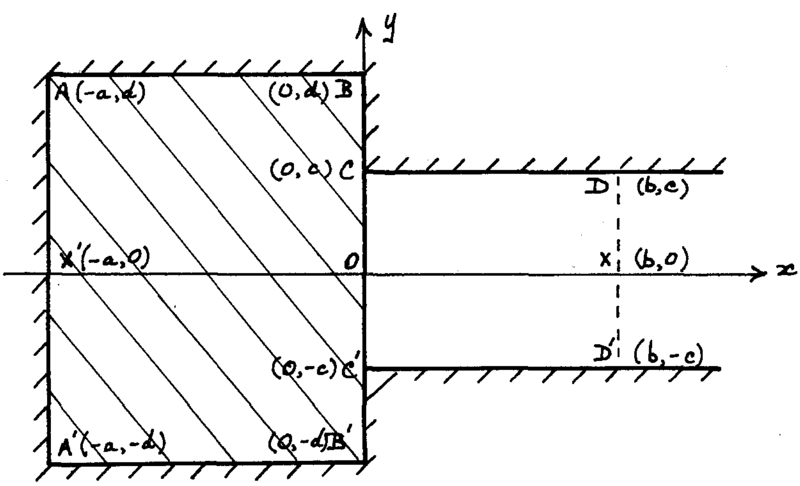

Figure 2. Rectangular conductor.

$H = H_y = I/(2c)$ and by implication $H_x = 0$. It would, therefore, appear to be desirable to choose a value $x = b > \xi$ to be a boundary and specify that there

$$H_y = -\frac{1}{\mu_0} \frac{\partial A}{\partial x} = \frac{I}{2c}\,; \quad H_x = \frac{1}{\mu_0} \frac{\partial A}{\partial y} = 0\,.$$

This implies that at $x = b$, A is a constant and thus it is desired to specify both the value of A and its normal derivative, and this leads to a mathematical problem which is overdefined. A choice has to be made between them and we follow Swann and Salmon in choosing to impose the condition on H_y, i.e. on the normal derivative, thus incorporating the fact that the total current is I. We differ from them in having the length b at our disposal whilst in their method b

was fixed as zero. This led to an inconsistency in that their expression for the current density J leads to a non-zero normal magnetic field strength over CC′. Our approach permits us to calculate the effective resistance and inductance and estimate the ratio of H_x/H_y at $x=b$ for various values of b. For a given conductor the minimum length of the neck of the slot for which the solution is acceptable is then obtained.

Then in CDD′C′

$$\nabla^2 A_1' = \nabla^2 A_1 = 0$$

and this equation can be solved by the same transform methods used in Section 2.2. It is only necessary to note that

$$\frac{dA_1^*}{dx}(x, 0) = \int_0^c \frac{\partial A_1}{\partial x} dx = -\mu_0 \int_0^c H_y dy = -\frac{\mu_0 I}{2}$$

so that A_1^* with $m=0$ is given by

$$A_1^*(x, 0) = cK - \frac{\mu_0 I}{2} x \tag{22}$$

to obtain the vector potential in the neck of the slot as

$$A_1 = K - \frac{\mu_0 I}{2c} x - \frac{2}{c} \sum_{m=1}^{\infty} \frac{P_m \cos(m\pi y/c)}{m\pi/c} \frac{\cosh\{(b-x)m\pi/c\}}{\sinh(bm\pi/c)} \tag{23}$$

and matching A_1, A_2 along the boundary as before, there results

$$Q_0 = \mu_0 I/2$$

$$Q_n - \frac{\mu_0 I}{2} \frac{\sin(n\pi c/d)}{n\pi c/d} + \frac{1}{c} \sum_{m=1}^{N} P_m k(m, n) = 0, \qquad n \neq 0 \tag{24}$$

$$cK + \frac{\mu_0 Ic}{2d\alpha_2} \coth(\alpha_2 a) + \frac{2}{d} \sum_{n=1}^{N} \frac{Q_n \sin(n\pi c/d) \coth(D_n a)}{D_n n\pi/d} = 0, \qquad m = 0 \tag{25}$$

$$\frac{P_m}{m\pi/c} \coth(m\pi b/c) = \frac{1}{d} \sum_{n=1}^{N} \frac{Q_n}{D_n} \coth(D_n a) k(m, n), \qquad m \neq 0 \tag{26}$$

Equations (24), (25), (26) provide $2N+1$ equations which may be solved for K, P_m $(1 \leqq m \leqq N)$, Q_n $(1 \leqq n \leqq N)$. Then use of Poynting's vector along CC′ yields, on carrying out the integration

$$R + jX = -\frac{j\omega}{I^2} \left\{ IK + \frac{4}{\mu_0 c} \sum_{m=1}^{N} \frac{|P_m|^2 \coth(bm\pi/c)}{m\pi/c} \right\}. \tag{27}$$

4. Some Computed Results

Designers of squirrel-cage induction motors are mainly interested in the effective resistance and reactance of the rotor bar. The internal impedance of a T-shaped conductor is given in equation (21), and of a rectangular conductor in equation (27). In both cases the Poynting vector was integrated over the surface of the conductor. The resulting reactance components are therefore associated with the slot leakage flux existing within the conductor and the impedance is termed "internal". The leakage flux in the air space in the slot neck above the rectangular conductor is not included. However, the influence of the possible 2-dimensional nature of the field in this region upon the field inside the conductor is taken into account by the solution.

In developing the formulae of the preceding sections the M.K.S. system of units has been employed and in using the method all dimensions must be in metres. In the following discussion however the dimensions of conductors and slots are given in millimetres.

4.1) *T-shaped Conductor.*
The r.m.s. phasor components of the magnetic field H_x and H_y are readily computed from equation (13) or equation (14) using the knowledge that

$$H_x = \frac{1}{\mu_0}\frac{\partial A}{\partial y} \quad \text{and} \quad H_y = -\frac{1}{\mu_0}\frac{\partial A}{\partial x}.$$

The instantaneous magnetic field components can then be obtained from the phasor quantities. For example

$$\begin{aligned} H_x(x, y, t) &= \mathrm{Re}[\sqrt{2}H_x e^{j\omega t}] \\ &= \mathrm{Re}[\sqrt{2}H_x]\cos\omega t - \mathrm{Im}[\sqrt{2}H_x]\sin\omega t. \end{aligned}$$

At the instant when the total current in the conductor ($\sqrt{2}I\cos\omega t$) is zero we can obtain the instantaneous field distribution by examining the imaginary parts of H_x and H_y alone. Figure 3 gives the distribution of the two components in the plane $x = -1$ mm. (see Figure 1), which is in the wide part of the conductor but close to the neck. Contrary to the usual assumption that the field is directed entirely across the slot, there is a substantial component H_x parallel to the

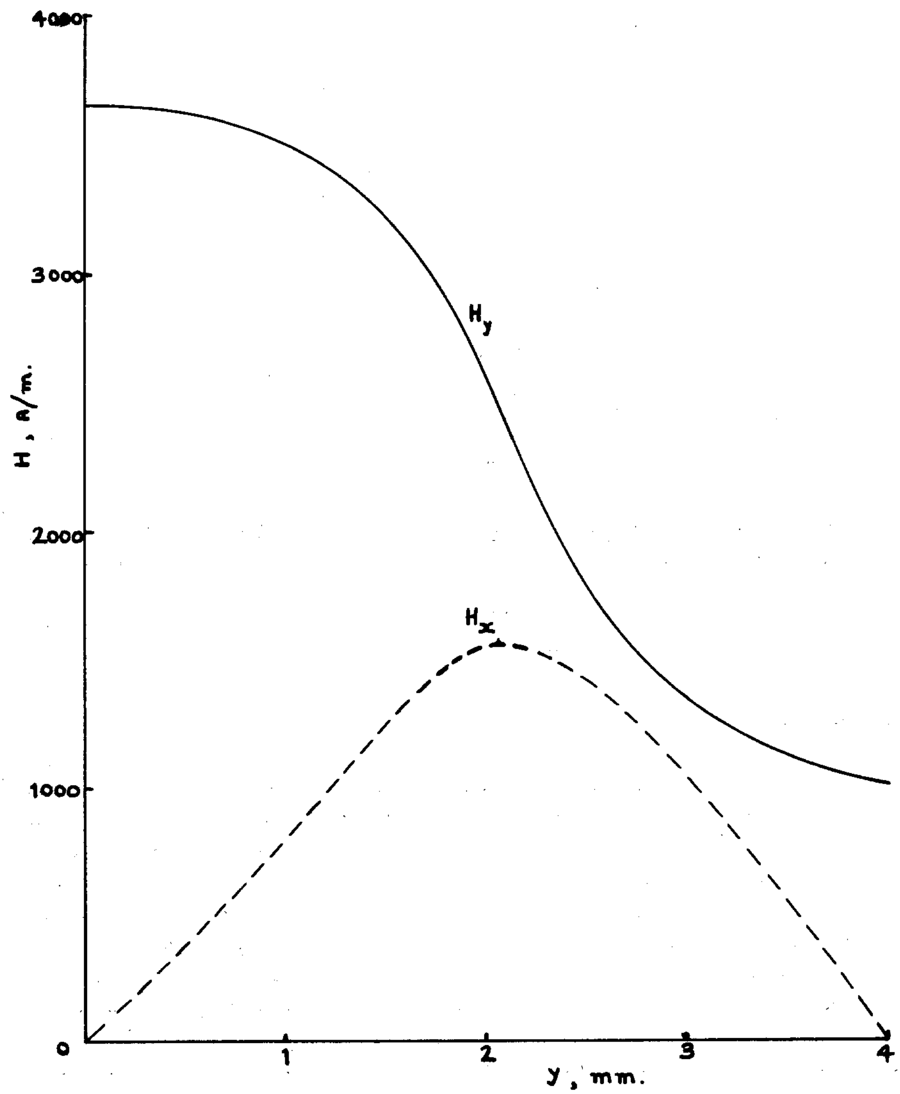

Figure 3. Field distribution in T-bar conductor; $a=20$ mm, $b=20$ mm, $c=2$ mm, $d=4$ mm, $x=-1$ mm, $I=100$ A, $f=40$ Hz.

centre line of the slot. The peak values of H_x occur at $y = \pm c$ where the bunching effect of the corner is greatest.

Putman's method of calculating resistance and inductance is widely used by designers. Since it is based on the assumption that H_x is zero everywhere the values of the effective resistance and inductance (R, L) obtained by the two methods are compared in Table 1 for four typical

TABLE 1
Resistance and inductance of T-shaped conductors

Conductor size (mm) & ref.	Frequency Hz	New method				Putman's method			
		R mΩ/m	L μH/m	R/R_0	L/L_0	R mΩ/m	L μH/m	R/R_0	L/L_0
$a = 17$	0.0001	0.05141	6.474	1.000	1.0000	0.05141	6.224	1.000	1.0000
$b = 25$	5	0.1127	5.567	2.191	0.8598	0.1070	5.472	2.081	0.8792
$c = 2$	10	0.2112	4.142	4.109	0.6397	0.2036	4.189	3.961	0.6730
$d = 8.5$	30	0.3969	2.034	7.720	0.3141	0.3997	2.047	7.774	0.3290
ref. A	50	0.4978	1.567	9.682	0.2420	0.4993	1.562	9.710	0.2509
$a = 10$	0.0001	0.06250	7.102	1.000	1.0000	0.06250	6.943	1.000	1.0000
$b = 35$	5	0.1405	5.451	2.247	0.7675	0.1372	5.452	2.195	0.7852
$c = 2$	10	0.2276	3.743	3.642	0.5270	0.2263	3.784	3.621	0.5450
$d = 9$	30	0.3850	2.028	6.160	0.2855	0.3853	2.022	6.165	0.2912
ref. B	50	0.4961	1.581	7.937	0.2227	0.4952	1.579	7.924	0.2274
$a = 7$	0.0001	0.08282	5.526	1.000	1.0000	0.08282	5.380	1.000	1.0000
$b = 28$	5	0.1293	4.907	1.561	0.8879	0.1259	4.847	1.521	0.9009
$c = 2$	10	0.2111	3.846	2.549	0.6959	0.2064	3.873	2.492	0.7200
$d = 9.25$	30	0.3915	2.032	4.727	0.3676	0.3934	2.037	4.751	0.3786
ref. C	50	0.4964	1.573	5.994	0.2847	0.4967	1.568	5.998	0.2915
$a = 15$	0.0001	0.07220	3.892	1.000	1.0000	0.07220	3.633	1.000	1.0000
$b = 13$	5	0.08737	3.814	1.210	0.9798	0.08452	3.578	1.171	0.9850
$c = 2$	10	0.1285	3.603	1.780	0.9259	0.1187	3.427	1.644	0.9432
$d = 7.5$	30	0.3624	2.436	5.020	0.6259	0.3379	2.476	4.680	0.6815
ref. D	50	0.5200	1.728	7.202	0.4439	0.5088	1.791	7.047	0.4928

conductors over a range of frequencies. Also included are the ratios R/R_0, L/L_0 where R_0, L_0 are the so-called static resistance and inductance. These are calculated at a very low frequency (0.0001 Hz.) so that R_0 is effectively the d.c. resistance. The values of L_0 are compared in Appendix 8.3 with those usually calculated at zero frequency on the assumption that the flux throughout the slot is unidirectional.

It will be seen from the results that Putman's values are reasonably accurate, the error being in the range $+1\%$, -5%.

It is at the low frequency that the maximum difference occurs between the inductance values calculated by the two methods. This is not surprising because, although the current distribution is uniform, the magnetic field in the slot is 2-dimensional. At higher frequencies the difference is less because the current is crowded into the narrow part of the conductor where the field is almost unidirectional.

On the other hand, the effective resistance depends entirely upon the current distribution and so, at the base frequency of 0.0001 Hz, the two methods agree exactly. This is again true for the higher frequencies. However, when there is a substantial part of the total current flowing in the broad part of the conductor Putman's method yields a low value for the resistance.

For all four conductors examined the ratio H_x/H_y at points along the top of the conductor at DD′ was found to be of order 10^{-10} or less. This approximates very closely the initial requirement that the magnetic field strength H_x along DD′ should be zero and so justifies the use of the method.

4.2) *Rectangular conductor.*

In this case a feature of major interest is the determination of the value to be chosen for b, the distance up the neck of the slot beyond which effectively

$$H_y = I/(2c), \quad H_x = 0\,.$$

Since at $x=b$

$$H_x = \frac{2}{\mu_0 c} \sum_{m=1}^{N} \frac{P_m \sin(m\pi y/c)}{\sinh(m\pi b/c)}$$

an upper bound to the ratio H_x/H_y is set by

$$U = \frac{4}{\mu_0 I} \sum_{m=1}^{N} \frac{|P_m|}{\sinh(m\pi b/c)} \geqq \frac{H_x}{H_y}\,.$$

Analytical investigation is hampered by the fact that P_m is not determined in analytic form. We, therefore, investigate numerically the effect of varying b with all other dimensions fixed and choose a conductor 8 mm wide and 20 mm deep with a slot opening of 4 mm (resistivity, $2 \cdot 10^{-8}$ Ω-m). For $b = 100$ mm the effective resistance and inductance are given in Table 2

TABLE 2

Frequency	New method $b = 100$ mm				Putman's method			
Hz	R mΩ/m	L μH/m	R/R_0	L/L_0	R mΩ/m	L μH/m	R/R_0	L/L_0
0.0001	0.12500	1.1941	1.0000	1.0000	0.12500	1.0459	1.0000	1.0000
5	0.12673	1.1900	1.0138	0.99652	0.12672	1.0418	1.0137	0.99608
10	0.13179	1.1779	1.0543	0.98643	0.13175	1.0298	1.0540	0.98459
30	0.17675	1.0724	1.4140	0.89803	0.17640	0.9246	1.4112	0.88400
50	0.23600	0.9388	1.8880	0.78618	0.23515	0.7914	1.8812	0.75663

TABLE 3

$b \cdot$ mm	0.001	0.01	0.1	1	10	10
L μH/m	0.9618	0.9604	0.9521	0.9390	0.9388	0.9388
Upperbound U	*	*	*	.11	10^{-7}	10^{-68}

* Not calculated since the series for U does not converge very quickly.

in comparison with the results achieved by Putman's method which is of course independent of the choice of b.

Since the major discrepancy occurs in the inductance the variation of this at 50 Hz was investigated for varying b. The results are given in Table 3 together with the upper bound U of $|H_x/H_y|$ at $x=b$.

Hence one can infer that the correct inductance is obtained if b is chosen to be greater than 1 mm, and in practice the neck length will usually fulfil this condition.

It is interesting to note that even with $b=0.001$ mm where it is not possible to asert that $H_x \ll H_y$ the error is less than 3 %. It was therefore considered pertinent to compare the result obtained by Swann and Salmon [2] for which b is chosen as zero. The use of the equation (their equation (33)) from which their curves were computed yielded a value of 1.263 μH/m. On investigating this discrepancy it was found that Swann and Salmon based their derivation of the internal impedance upon the electric field strength in the conductor surface at the centre of the slot opening. However the current density, and hence electric field, vary across the surface. It is therefore suggested that a Poynting integral would be more appropriate, a view shared by Annell [6]. This leads to k_n^2 in place of k_n in the series of their equation (27). On arriving at their equation (33) from which the curves were computed an error in transcription seems have led to the introduction of an unwanted factor of 2 into the series so that the corrected version of their equation (33) is, in their notation,

$$\frac{X_e}{R_d}=\frac{b}{\delta}\left(\frac{\sinh(2b/\delta)-\sin(2b/\delta)}{\cosh(2b/\delta)-\cos(2b/\delta)}+\frac{4b}{\delta}\sum_{n=1}^{\infty}\frac{\sin^2(n\pi l/a)}{(n\pi l/a)^2}\,\frac{\coth(n2\pi b/a)}{n2\pi b/a}\right)$$

For our example this yields an inductance of 0.9666 μH/m in close agreement with the result $b=0.001$ mm in Table 3.

5. Conclusions

An analytical method, suitable for automatic computation, has been developed for calculating the internal impedance of, and the magnetic field and current distribution in, T-shaped conductors in electrical machine slots. Impedance calculations on typical conductors have shown that the simpler method of Putman [1], who assumed that the flux goes straight across the slot, is adequate if an error of the order of 5 % is acceptable.

A similar solution has been obtained for rectangular conductors. In this case Putman's assumption can lead to large errors in the inductance, of the order of 15 % in the example chosen. The method removes the restricting assumption that the top of the conductor is bounded by a flux line [2]. However this assumption affects the inductance only by 3 % in the example chosen.

6. Acknowledgements

The authors wish to thank Mr. G. Campbell of C. A. Parsons Ltd., for helpful discussions and the Magnet Computer Bureau Ltd., for permission to offer the paper for publication.

7. Appendix

7.1) Determination of the coefficients P_m, Q_n

Equations (15), (16) and (17) are available for the determination of the $2N+2$ unknowns (P_m, $0\leqq m\leqq N$; Q_n, $0\leqq n\leqq N$) and can be written in the form:

$$\begin{bmatrix} I_{1,1} & 0_{1,N} & S_0 & S_{1,N}\\ 0_{N,1} & I_{N,N} & 0_{N,1} & V_{N,N}\\ W_0 & 0_{1,N} & I_{1,1} & 0_{1,N}\\ W_{N,1} & U_{N,N} & 0_{N,1} & I_{N,N}\end{bmatrix}\begin{bmatrix}P_0\\ P_{N,1}\\ Q_0\\ Q_{N,1}\end{bmatrix}=\begin{bmatrix}X_0\\ 0_{N,1}\\ 0_0\\ 0_{N,1}\end{bmatrix}$$

where a single subscript denotes a scalar and a double subscript i,j say denotes a matrix of order $i\cdot j$.

For example: $P_{N,1}=\mathrm{col}\{P_1, P_2, \ldots, P_N\}$, $I_{j,j}$ is a unit matrix of order j, $0_{i,j}$ is a zero matrix of order $i\cdot j$.

This matrix may be reduced as follows:

(a) Pre-multiply row 3 by S_0, row 4 by $S_{1,N}$ and subtract from row 1.

(b) Pre-multiply row 4 by $V_{N,N}$ and subtract from row 2 to obtain

$$\begin{bmatrix} I_{1,1}-S_0W_0-S_{1,N}W_{N,1} & -S_{1,N}U_{N,N} & 0_0 & 0_{1,N}\\ -V_{N,N}W_{N,1} & I_{N,N}-V_{N,N}U_{N,N} & 0_{N,1} & 0_{N,N}\\ W_0 & 0_{1,N} & I_{1,1} & 0_{1,N}\\ W_{N,1} & U_{N,N} & 0_{N,1} & I_{N,N}\end{bmatrix}\begin{bmatrix}P_0\\ P_{N,1}\\ Q_0\\ Q_{N,1}\end{bmatrix}=\begin{bmatrix}X_0\\ 0_{N,1}\\ 0_0\\ 0_{N,1}\end{bmatrix}$$

Now writing $Z_{N,N}=[I_{N,N}-V_{N,N}U_{N,N}]^{-1}$ pre-multiply row 2 by $Z_{N,N}$. Further pre-multiply row

2 by $S_{1,N}U_{N,N}$, subtract from row 1 and reduce the first term of row 1 to unity giving:

$$\begin{bmatrix} I_{1,1} & 0_{1,N} & 0_0 & 0_{1,N} \\ -Z_{N,N}V_{N,N}W_{N,1} & I_{N,1} & 0_{N,1} & 0_{N,N} \\ W_0 & 0_{1,N} & I_{1,1} & 0_{1,N} \\ W_{N,1} & U_{N,N} & 0_{N,1} & I_{N,N} \end{bmatrix} \begin{bmatrix} P_0 \\ P_{N,1} \\ Q_0 \\ Q_{N,1} \end{bmatrix} = \begin{bmatrix} X_0' \\ 0_{N,1} \\ 0_0 \\ 0_{N,1} \end{bmatrix}$$

where

$$X_0' = \frac{X_0}{I_{1,1} - S_0 W_0 - S_{1,N} W_{N,1} - S_{1,N} U_{N,N} Z_{N,N} V_{N,N} W_{N,1}}$$

from which P_0; $P_{N,1}$; Q_0; $Q_{N,1}$ follow in order to yield:

$$\begin{aligned} P_0 &= X_0' \\ P_{N,1} &= X_0' Z_{N,N} V_{N,N} W_{N,1} \\ Q_0 &= -X_0' W_0 \\ Q_{N,1} &= -X_0' [I_{N,N} + U_{N,N} Z_{N,N} V_{N,N}] W_{N,1} \end{aligned}$$

It will be noted that this involves the inversion of only one $N \cdot N$ matrix and considerably reduces the computation involved.

7.2) *Truncation of the Series.*

The series expressions must be truncated at some number of terms N before the solution can be computed. The change in the impedance was found to be negligible when N was varied between 5 and 20. 10 terms were thus taken for all impedance calculations. On the other hand, calculation of the magnetic field at points inside the conductor may require 20 terms, or even more, close to the restriction at $x = 0$.

7.3) *The d.c. inductance.*

At zero frequency the current density is constant over the cross-section of the conductor and the d.c. internal inductance is usually calculated by making the assumption that the flux is entirely directed across the slot. Then flux density is given by

$$B = \begin{cases} \mu_0 I \dfrac{x}{2(ad+bc)} & \text{for } 0 < x < a \\[2ex] \dfrac{\mu_0 I}{2(ad+bc)} \left\{ \dfrac{ad}{c} + x - a \right\} & \text{for } a < x < b\,, \end{cases}$$

where x is now the distance from the base of the slot.

In calculating the internal inductance it is the flux linkage of this flux which is required. The flux linkage with an element of length dx (and height $2d$) in the region ABB′A′ of Figure 1 is

$$d\Omega_1 = \left\{ \frac{\mu_0 I}{2(ad+bc)} \int_x^a \xi \, d\xi + \frac{\mu_0 I}{2} \frac{b}{c} \left(1 - \tfrac{1}{2} \frac{bc}{ad+bc} \right) \right\} \frac{d}{ad+bc} dx$$

and for an element of length dx (and height $2c$) in the region CDD′C′

$$d\Omega_2 = \left\{ \frac{\mu_0 I}{2(ad+bc)} \int_x^{a+b} \left(\frac{ad}{c} + \xi - a \right) d\xi \right\} \frac{c}{ad+bc} dx\,.$$

On carrying out the integrations w.r.t. ξ and then w.r.t. x there results

$$L_0 = \frac{\Omega_1 + \Omega_2}{I} = \frac{\mu_0}{2(ad+bc)^2} \left\{ \frac{a^2 bd^2}{c} + ab^2 d + \frac{a^3 d}{3} + \frac{b^3 c}{3} \right\}. \tag{28}$$

The internal d.c. inductance of the rectangular bar may be obtained by putting $b = 0$ in equation 28.

These approximate d.c. values are compared in Table 4 with those calculated at 0.0001 Hz both by the new method and by Putman's method.

TABLE 4

Conductor Ref.	Approx. d.c. inductance μH/m	Inductance L_0 at 0.0001 Hz. New method	Putman' method
A	6.237	6.474	6.224
B	6.961	7.102	6.943
C	5.436	5.526	5.380
D	3.699	3.892	3.633
Rectangular	1.0472	1.1941	1.0459

Comparison of the d.c. inductances and those at 0.0001 Hz by Putman's method show a small fall due to the frequency. Both however depend on the assumption that the flux is unidirectional. This restriction is removed in the new method and, assuming that here too the frequency gives rise to a small fall, it is apparent that the true d.c. inductance can considerably exceed the approximate value usually used. Indeed for the rectangular conductor investigated the error is 13 %.

REFERENCES

[1] H. V. Putman; Starting Performance of Synchronous Motors, *A.I.E.E., J*, 46, pp. 794–801, 1927.
[2] S. A. Swann and J. W. Salmon; Effective resistance and reactance of a rectangular conductor in a semi-closed slot, *Proc. I.E.E.*, 110(9), pp. 1656–1662, 1963.
[3] D. Midgley and S. W. Smethurst; Magnetic field problem with axial symmetry, *Proc. I.E.E.*, 110(8), pp. 1465–1472, 1963.
[4] P. Silvester; Dynamic resistance and inductance of slot-embedded conductors, *I.E.E.E. Trans., P.A.S.*, 87(1), pp. 250–256, 1968.
[5] J. Irving and N. Mullineux; *Mathematics in Physics and Engineering*, Academic Press, 1959.
[6] H. Annell; The a.c. impedance of a solid conductor of circular cross-section placed in a semi-closed slot, *Trans. Roy. Inst. Tech.*, Stockholm, *Elec. Eng.*, 9, No. 200, 1963.

Journal of Engineering Math., Vol. 3 (1969) 123–135